Differential conductance anomaly in superconducting quantum point contacts

Argo Nurbawono,[1] Yuan Ping Feng,[1] Erhai Zhao,[2,1] and Chun Zhang[1,3,*]
[1]*Department of Physics, National University of Singapore, 2 Science Drive 3, Singapore 117542, Singapore*
[2]*Department of Physics and Astronomy, George Mason University, Fairfax, Virginia 22030, USA*
[3]*Department of Chemistry, National University of Singapore, 3 Science Drive 3, Singapore 117543, Singapore*
(Received 28 October 2009; published 30 November 2009)

We present in this paper a theoretical analysis of the current-voltage (*I-V*) characteristics of a hybrid normal-superconducting device consisting of a quantum dot and two electrodes that can be either normal or superconducting. We show that voltage drops at two different contacts that have been regarded unimportant in literature play essential roles in the Andreev tunneling process when at least one of electrodes is superconducting. A differential-conductance anomaly caused by the aforementioned voltage drops is predicted. We also propose a spectroscopy method to measure the energy levels of a quantum dot as well as voltage drops at contacts between the quantum dot and the two leads. Our findings have potential applications for the next generation of electronic devices at nanoscale.

DOI: 10.1103/PhysRevB.80.184516 PACS number(s): 73.40.Gk, 74.45.+c, 73.63.Rt, 74.50.+r

I. INTRODUCTION

Transport through a superconducting quantum point contact (QPC), a normal (N) atomic or molecular-size center characterized by several discrete energy levels, and connected to two superconducting (S) electrodes, plays a fundamental role in our understanding of nanoelectronic devices driven out of equilibrium, thanks to the ac-Josephson effect.[1] Two widely used techniques to fabricate QPCs are scanning tunneling microscope (STM)[2] and mechanically controlled break-junctions (MCBJs).[3] They often operate at low temperatures so that the two electrodes are in the superconducting phase. The measured current-voltage (*I-V*) characteristics for a superconducting QPC often shows a linear behavior at "high" bias voltages ($\sim 3\Delta/e$, Δ is the superconducting gap), and a complicated subgap structure at low bias originating from multiple Andreev reflections (MARs).[4–6] The differential conductance in the linear range of the *I-V* curve is believed to be the same as the normal junction,[3,7–9] and the subgap structure can be used to identify the transmission eigenchannels of the normal junction via the so-called PIN code.[10] Recently, these superconducting *I-V* characteristics have been employed to probe other internal degrees of freedom of the atomic center such as magnetic structures,[2,11] molecular vibrating modes,[8] and Kondo impurity.[12]

In theoretical modeling, the atomic center can be modeled by a quantum dot, and voltage drops at two contacts between the electrodes and the center quantum dot are conventionally assumed to be the same, i.e., half of the bias voltage[11,13] which may be justified for symmetric electrodes or for small bias voltage (in the linear-response regime). For real molecular junctions, the nature of bonding at two contacts is usually different which may result in different voltage drops. This has dramatic consequences on the transport properties especially for superconducting electrodes. Even a small difference between these two voltage drops ($\sim\Delta/e$), which would be unimportant for normal junctions will significantly shift the position of energy levels of the quantum dot relative to superconducting gap edges to cause substantial changes in MAR processes. Despite their importance, these issues have not been investigated before.

In this paper, we present theoretical results on the nonequilibrium transport properties of a quantum dot connected to two electrodes that can be either normal or superconducting. Our focus is on the effect of the symmetry, or lack of it, between the two contacts on the renormalization of the dot energy levels and the tunneling processes. We show that the aforementioned connections between *I-V* curves of superconducting QPCs and transport properties of normal ones become complicated for general contacts symmetry. However, these "complications" can be turned into a useful spectroscopic tool for QPCs such as molecular nanojunctions.

II. MODEL AND METHOD

The model system under study is shown in Fig. 1(a), where a quantum dot is connected to two electrodes and the whole system is under a bias voltage V. The voltage drops from the left electrode to the quantum dot, and from the dot to the right electrode are denoted as V_{LD} and V_{DR} respectively. The Hamiltonian of the system can then be written as

$$H = H_L + H_R + H_D + H_T, \tag{1}$$

where the Hamiltonian for the left (right) lead $H_{L(R)}$ in the framework of Bardeen-Cooper-Schrieffer (BCS) theory, quantum dot H_D, and tunneling term H_T are given by

$$H_L + H_R = \sum_{k,\sigma,\alpha=L,R} \epsilon_{\alpha,k,\sigma} a^{\dagger}_{\alpha,k,\sigma} a_{\alpha,k,\sigma} + \sum_{k,\alpha} \Delta_{\alpha} a_{\alpha,k,\downarrow} a_{\alpha,-k,\uparrow} + \text{H.c.}, \tag{2}$$

$$H_D = \sum_{d,\sigma} (\epsilon_{d,\sigma} - eVs) c^{\dagger}_{d,\sigma} c_{d,\sigma}, \tag{3}$$

$$H_T = \sum_{k,d,\sigma,\alpha=L,R} t_{\alpha,d} e^{i/2(\phi_{\alpha}+2/\hbar eV_{\alpha}t)} a^{\dagger}_{\alpha,k,\sigma} c_{d,\sigma} + \text{H.c.} \tag{4}$$

In this paper, we assume that the two BCS superconducting leads are symmetric so that the superconducting gap of left

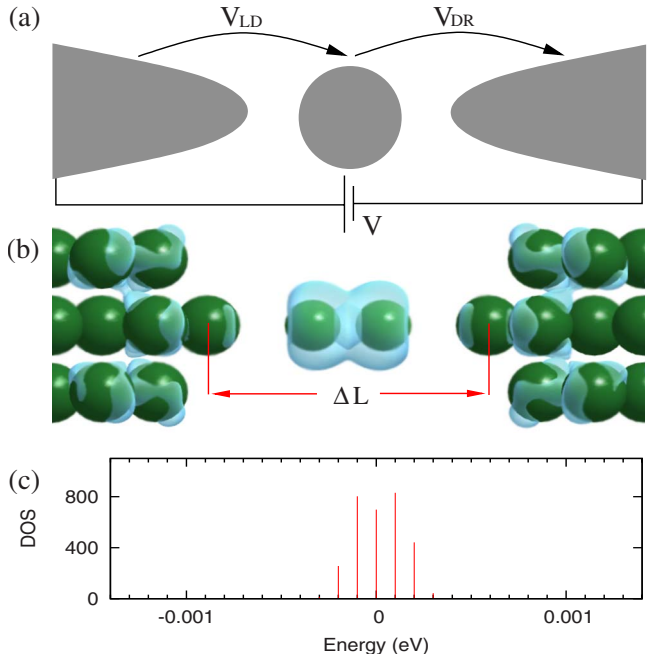

FIG. 1. (Color online) (a) Sketch of potential drop across the central region: $V_{LD}+V_{DR}=V$, and in general $V_{LD}\neq V_{DR}$. (b) Bcc (100) Nb leads connected by an Nb dimmer. The distance between two tips, $\Delta L=8.2$ Å, is consistent with the Ref. 8. The iso-surface of electron density around Fermi energy is also shown. (c) Total DOS from DFT calculation resolved up to 0.1 meV, showing states around the fermi energy.

lead is the same as that of right lead, $\Delta_L=\Delta_R=\Delta$. Through out the paper, the left lead is taken to be the potential ground, so we have $V_L=0$, and the bias voltage V equals $-V_R$. The initial superconducting phases of two leads are denoted as $\phi_{L,R}$. Energy levels in the quantum dot are denoted as $\epsilon_{d,\sigma}$ where σ is the spin index. The 'symmetry' parameter s in H_D is defined as $s=V_{LD}/V$, and the term $-eVs$ represents the potential shift of the quantum dot due to the distribution of bias voltage at two contacts. Note that this potential shift is bias dependent; therefore, it is very different from the constant potential shift due to gate voltage. In literature, s is usually set to be 0.5 corresponding to the same voltage drops at two contacts.[11,13] In current work, we examined the effects of different s on the tunneling of the supercurrent. A real example of the QPC is shown in Fig. 1(b), where two superconducting bcc (100) Nb leads are connected by a Nb dimer. This Nb junction has been shown by recent studies to correspond to Nb contacts fabricated by MCBJ method in experiments.[7,8] The atomic configuration of the junction is determined by first pinciples calculations based on density-functional theory (DFT),[14] and consitent with the reference 8. The density of states (DOS) calculated by DFT method is shown in Fig. 1(c), where several localized states near the Fermi energy can be clearly seen. In Fig. 1(b),we also show the isosurface of the electron density near the Fermi energy (from E_f-1 meV to E_f+1 meV), where we can see that those states are indeed localized on the Nb dimer. Since the difference between the localized state and the Fermi energy is smaller than the superconducting gap of Nb ($\sim$1.4 meV), the Nb dimer can be treated as a quantum dot with several localized levels inside the superconducting gap, and can be described by Hamiltonian in Eq. (1). It is worth mentioning here that unlike the macroscopic quantum dot for which the parameter s may be a simple function of Γ_L and Γ_R, the system we are interested in is very small (at molecular scale). For such small systems, the potential drops at two contacts sensitively depend on chemical bonding; therefore an explicit expression for s is not possible, and it has to be calculated self consistently by first-principles method. When a finite bias is applied to the system, potential drops at two contacts can be evaluated by solving Poisson's equation under the framework of the *ab initio* method combining density-functional theory and nonequilibrium Green's function's techniques.

The coupling term H_T in Eq. (1) is a function periodic in time with a frequency $\omega=2eV/\hbar$. Therefore, the time-dependent current $I(t)$ is also periodic in time, and has a discrete Fourier transform as the following:

$$I(t)=\sum_n I_n e^{in\omega t}. \tag{5}$$

The time-averaged current $I_0(t)=\int j_0(\epsilon)d\epsilon$, where $j_0(\epsilon)$ is the current density that can be evaluated in terms of Green's functions of quantum dot[15] as

$$I_0=-\frac{e}{\pi}\int \mathrm{Im}\left\{\mathrm{Tr}\left\{\left[f_L(\epsilon)\rho_L(\epsilon)G^r_{m,n=0}(\epsilon)+\frac{1}{2}\beta^*_L(\epsilon)G^<_{m,n=0}(\epsilon)\right]\Gamma_L\Sigma_L\sigma_z\right\}\right\}d\epsilon. \tag{6}$$

In Eq. (6), $G^{r(<)}_{m,n}(\epsilon)$ denotes the double Fourier transform of retarded (lesser) Green's function of the quantum dot in Nambu space.[13] The term $f_L(\epsilon)$ is the left lead Fermi-Dirac distribution function. $\rho_L(\epsilon)$ is the BCS density of states of left lead (the normal density of states of the lead is taken to be 1), and can be calculated by $\rho_L(\epsilon)=\mathrm{Re}(\beta_L(\epsilon))$, where $\beta_{L/R}(\epsilon)=-i\epsilon/\sqrt{\Delta^2_{L/R}-\epsilon^2}$ for $\Delta_{L/R}>|\epsilon|$, and $\beta_{L/R}(\epsilon)=|\epsilon|/\sqrt{\epsilon^2-\Delta^2_{L/R}}$ for $\Delta_{L/R}<|\epsilon|$. Σ and σ_z are self-energy of leads and Pauli matrix, respectively. The coupling function $\Gamma_{L/R}$ is defined as $\Gamma_{L/R,ij}=2\pi t_{L/R,i}t^*_{L/R,j}$. In the paper, Γ_L and Γ_R are assumed to be two constants. The retarded Green's function can be computed by Dyson equation via direct matrix inversion, $G^r_{m,n}(\epsilon)=[(g^r)^{-1}-\Sigma^r]^{-1}$, where g^r is the double Fourier transform of retarded Green's function of bare quantum dot without two leads, and Σ^r is the summation of retarded self energies of two leads. With G^r, the lesser Green's function can be calculated as $G^<_{m,n}(\epsilon)=[G^r(\epsilon)\Sigma^<(\epsilon)G^a(\epsilon)]_{m,n}$, where $\Sigma^<=\Sigma^<_L+\Sigma^<_R$. $\Sigma^<_{L(R)}$ is the lesser self-energy of left (right) lead. The double Fourier transforms of g^r, Σ^r, and $\Sigma^<$ in Nambu space are calculated in standard way.[15]

III. RESULTS AND DISCUSSION

For simplicity, we first consider a quantum dot with only one level $\epsilon_d=0.0$ eV, neglect spin-dependence, and assume $\Gamma_L=\Gamma_R=\Gamma$. In Fig. 2(a), the time-averaged S-N-S current as a function of bias voltage for $s=0.5$ and 0.2 is shown

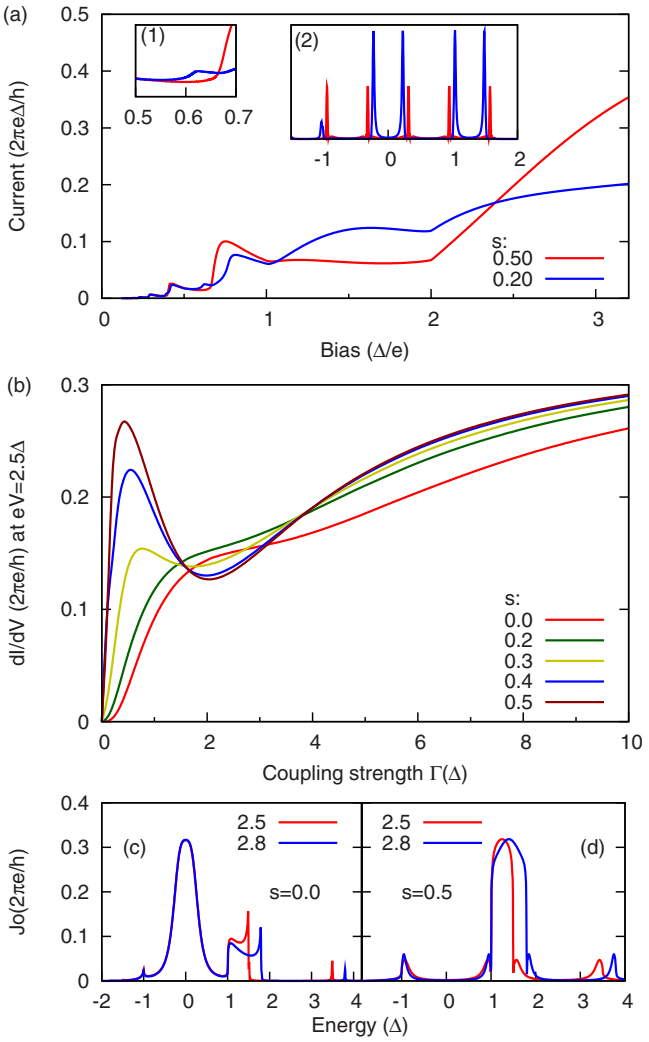

FIG. 2. (Color online) (a) Time averaged I-V curves for two different s calculated at $\Gamma=0.5\Delta$, $\epsilon_d=0$ ($k_bT=0.1\Delta$ for all graphs). Inset (1): The small peak around $eV=0.63\Delta$. Inset (2): Current density as a function of energy for the bias voltage $eV=0.63\Delta$. Each peak inside the gap corresponds to one current-carrying Andreev bound state. Note that there are five Andreev bound states for $s=0.5$, and only four for $s=0.2$. (b) dI/dV as a function of coupling strength Γ for various s. A peak appears around $\Gamma\sim0.5\Delta$ for $s>0.3$. Time averaged current density J_0 as a function of energy at two slightly different bias, $eV=2.5\Delta$ and $eV=2.8\Delta$, for (c) $s=0.0$, and (d) $s=0.5$.

($\Gamma=0.5\Delta$ in calculations). For $s=0.5$, the I-V curve shown in the figure essentially is the same as that calculated by Yeyati[13] although the method we used here is different. When bias voltage is small ($eV<0.5\Delta$), the I-V curve is not sensitive to s, while for bigger bias voltages, we see significant differences between I-V curves for different s. For subgap structures ($eV<2\Delta$), both positions and heights of peaks of I-V curves for different s are different. Furthermore, a small "new" peak appears around $eV\approx0.63\Delta$ when $s=0.2$. This small peak is caused by subtle effects of s on positions of Andreev bound states. The current density as a function of energy at bias voltage 0.63Δ is shown in inset (2) of the figure. When $s=0.5$, the dot level exactly lies in the middle of superconducting gaps, and symmetrically couples to left and right superconducting gaps, leading to evenly distributed current-carrying Andreev bound states (ABSs) inside the gap as shown in the figure. Note that when $s=0.5$, there are five ABSs, and the spacing between successive states is exactly 0.63Δ. When s changes from 0.5 to 0.2, the dot level is shifted leftward (becoming less), and the leftmost ABS is shifted leftward also. This shift drives the ABS outside the superconducting gap, and in turn greatly supresses the state due to the absense of MAR outside the gap, resulting in only four ABSs inside the gap for $s=0.2$. The decrease of the number of ABSs inside the gap means the decrease in total number of Andreev reflections, leading to the increase of total current as we can see from the significant increase of the current density each ABS carries for $s=0.2$. When bias voltage is slightly increased, the leftmost peak of $s=0.2$ will be further away from the gap, leading to greater supression of the state and the small decrease of total current. At bias voltages bigger than $2\Delta/e$, the I-V curve is linear regardless of s, while, the differential conductance changes drastically when s changes. In order to see effects of s on I-V characteristics more clearly, we plot the differential conductance dI/dV as function of Γ at bias voltage $2.5\Delta/e$ for different values of s in Fig. 2(b). Since two leads are symmetric, there are no differences in I-V characteristics between s and $(1-s)$, so we only show cases for $s\leq0.5$. For all s smaller than 0.3, dI/dV as a function of Γ is essentially the same. It decreases monotonically with Γ, and resembles dI/dV in the linear-response regime of a quantum dot connected with two normal leads, $dI/dV\propto\Gamma^2/[\epsilon_d^2+\Gamma^2]$,[16] where ϵ_d is the energy level of the dot. This supports the general belief in previous theoretical and experimental studies[2,3,7,8,10] that dI/dV of a superconducting QPC measured at a 'high' bias around $2.5\Delta/e$ can be taken to be the conductance of the corresponding normal QPC. However, when s increases, at small coupling ($\Gamma<2\Delta$), dI/dV starts to significantly deviate from the linear-response behavior of normal junctions. For the case of symmetrical contacts ($s=0.5$), a high differential-conductance peak appears at small Γ around 0.5Δ. The peak value is quite high that it is comparable to the conductance at big Γ around 10Δ. This is certainly very surprising and will never occur for normal junctions.

This differential-conductance anomaly can be understood by the broadening of the energy level of the quantum dot due to coupling with two superconducting leads. At a "high" bias voltage ($\sim2.5\Delta/e$), the time-averaged electron DOS of the quantum dot can be simplified to

$$\mathrm{DOS}(\epsilon)=\frac{1}{\pi}\frac{\frac{\Gamma}{2}\mathrm{Re}(z)}{[\epsilon-(\epsilon_d-eVs)]^2+\left[\frac{\Gamma}{2}\mathrm{Re}(z)\right]^2}, \tag{7}$$

where $z=\beta(\epsilon)+\beta(\epsilon+V)$. When $s=0.0$, the energy level of the quantum dot is pinned at the center of superconducting gap of the left lead. The broadening of the energy level due to coupling with two leads, $\Gamma/2\ \mathrm{Re}(z)$, in this case is approximately Γ which is independent on bias. When the coupling strength Γ is less than the width of the gap (Δ), the dot level

is completely confined within the gap. When $s=0.5$, the dot level lies between two superconducting gaps, and the broadening is a function of bias.

To see the connection between DOS and dI/dV, we calculated the current density as a function of energy for $\Gamma=0.5\Delta$ at bias voltages $2.5\Delta/e$ and $2.8\Delta/e$ for both $s=0.5$ and $s=0.0$ as shown in Figs. 2(c) and 2(d). At bias voltages $\sim 2.5\Delta/e$, the current tunneling through the dot level dominates the total current, and the dominating current-density peak shows the similar behavior as that of DOS as we can see in the figure. When $s=0.0$ [Fig. 2(c)], the dominating peak is completely confined inside the left superconducting gap, and remains the same when the bias voltage changes from $2.5\Delta/e$ to $2.8\Delta/e$, resulting in a small differential conductance. When $s=0.5$ [Fig. 2(d)], the dominating peak lies between two superconducting gaps, and the half width is essentially determined by the energy window defined as the distance between nearest boundaries of two gaps. As a result, when the bias changes from $2.5\Delta/e$ to $2.8\Delta/e$, the current-density peak originating from tunneling through the dot level becomes much broader, leading to a much bigger current and a high differential conductance. When two leads are normal, $\mathrm{Re}(z)$ in Eq. (7) is 2, and the broadening of the dot level is simply Γ, which is independent on bias voltage, and the differential-conductance anomaly will not occur.

We then calculated dI/dV as a function of Γ_L at $eV=2.5\Delta$ for a two-level quantum dot with different values of Γ_R, and found essentially the same physics: A high differential-conductance peak appears at small Γ_L around 0.5Δ for $s>0.3$. For a microscopic quantum point contact, s is mainly determined by the bonding nature at two contacts, and may be tuned via the nice control of the distance between the quantum dot and two leads in MCBJs or junctions made by STM. Also, since the coupling function, $\Gamma_{L/R}$, sensitively depends on the distance between two leads, we believe that with a nice control of the breaking process of the junction, the differential-conductance-anomaly discussed here should be able to be observed in experiment.

We next examine the effects of s on transport properties of an S-N-N junction. In our calculations, we set the left lead to be superconducting, and the right lead to be normal by taking $\Delta_R=0$. In this case, the tunneling term H_T in Eq. (4) has no time dependence. Therefore, the double Fourier transform is not needed.[19] Following the similar procedure as described above, the current tunneling through the S-N-N junction can be calculated using Eq. (6). In Fig. 3(a), we show I-V curves for different s when the dot level is zero. In this case, I-V curves are antisymmetric for positive and negative biases. When the dot level is not zero, for example $\epsilon_d=0.5\Delta$, the antisymmetry between positive and negative biases is absent, and a peak appears at a certain positive bias that is a function of s as shown in Fig. 3(b). The peak of the current is a result of the resonance tunneling when $\epsilon_d=eV_ps$, where V_p is the bias voltage at which the resonance occurs. With the help of a gate voltage which shifts the dot energy level, the peak of the I-V curve can be used to measure the dot level ϵ_d and the symmetry factor s. First, without gate voltage, we have $\epsilon_d=eV_ps$, where V_p is the bias voltage

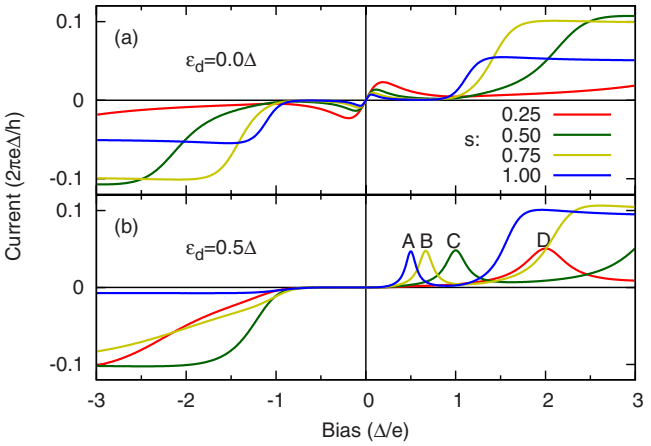

FIG. 3. (Color online) I-V curve for S-N-N junction for different values of s: (a) $\epsilon_d=0\Delta$, (b) $\epsilon_d=0.5\Delta$. Peaks of I-V curves in (b) are at bias voltages (in unit of Δ/e): $A=0.50$, $B=0.67$, $C=1.00$, and $D=2.00$.

where we get a peak in I-V curve. Then with a gate voltage V_g applied to the quantum dot, we have $\epsilon_d+eV_g=eV_p's$, where V_p' is the new peak position with the gate voltage. Comparing these two equations, we have $s=V_g/(V_p'-V_p)$ and then the dot level can be computed. This technique is also applicable to the dot with multilevels, where we have multipeaks in I-V curves with each of them corresponding to one dot level (not shown in this paper).

IV. SUMMARY

In summary, we presented in this paper a systematic theoretical analysis for transport properties of S-N-S and S-N-N QPCs. We demonstrated that for superconducting QPCs, the voltage drops at two contacts play essential roles in the supercurrent tunneling. When two contacts are symmetric, i.e., voltage drops are the same at two contacts, a differential-conductance anomaly at small Γ for bias voltages higher than $2\Delta/e$ is predicted. This differential-conductance anomaly is caused by the broadening of the energy level in quantum dot due to the coupling with two superconducting leads, and will not occur for normal junctions. For S-N-N junctions, we suggested that the peak of I-V curve can be used to measure the dot level and the symmetry factor s which provides information of voltage drops at two contacts. We believe that the spectroscopy method proposed here has important potential applications for molecular electronics where the junction is usually molecular scale, and direct measurements of voltage drops at contacts are in principle forbidden since a small perturbation, i.e., the addition of a small molecule, will destroy the junction.

ACKNOWLEDGMENTS

This work was supported by NUS Academic Research Fund (Grants No. R-144-000-237133 and No. R-144-000-255-112). Computations were performed at the Centre for Computational Science and Engineering at NUS.

*phyzc@nus.edu.sg

[1] B. D. Josephson, Rev. Mod. Phys. **36**, 216 (1964).
[2] S. H. Ji, T. Zhang, Y. S. Fu, X. Chen, X. C. Ma, J. Li, W. H. Duan, J. F. Jia, and Q. K. Xue, Phys. Rev. Lett. **100**, 226801 (2008).
[3] C. J. Muller, J. M. van Ruitenbeek, and L. J. de Jongh, Phys. Rev. Lett. **69**, 140 (1992).
[4] M. Octavio, M. Tinkham, G. E. Blonder, and T. M. Klapwijk, Phys. Rev. B **27**, 6739 (1983).
[5] E. N. Bratus', V. S. Shumeiko, and G. Wendin, Phys. Rev. Lett. **74**, 2110 (1995).
[6] D. V. Averin and A. Bardas, Phys. Rev. Lett. **75**, 1831 (1995).
[7] A. Marchenkov, Z. Dai, C. Zhang, R. N. Barnett, and U. Landman, Phys. Rev. Lett. **98**, 046802 (2007).
[8] A. Marchenkov, Z. Dai, B. Donehoo, R. N. Barnett, and U. Landman, Nat. Nanotechnol. **2**, 481 (2007).
[9] P. Makk, Sz. Csonka, and A. Halbritter, Phys. Rev. B **78**, 045414 (2008).
[10] E. Scheer, P. Joyez, D. Esteve, C. Urbina, and M. H. Devoret, Phys. Rev. Lett. **78**, 3535 (1997); J. C. Cuevas, A. Levy Yeyati, and A. Martin-Rodero, *ibid.* **80**, 1066 (1998).
[11] E. Zhao and J. A. Sauls, Phys. Rev. Lett. **98**, 206601 (2007); Phys. Rev. B **78**, 174511 (2008).
[12] Y. Tanaka, A. Oguri, and A. C. Hewson, New J. Phys. **9**, 115 (2007).
[13] A. Levy Yeyati, J. C. Cuevas, A. Lopez-Davalos, and A. Martin-Rodero, Phys. Rev. B **55**, R6137 (1997).
[14] In the structure optimization, two outermost layers of the junction are fixed to the bulk Nb structure, and only the contact region as shown in Fig. 1 is allowed to relax. The DFT calculations include the generalized gradient approximation,[17] using a plane-wave basis (kinetic-energy cutoff 210 eV) and projector augmented-wave pseudopotential.[18] More details can be found in our previous study.[7]
[15] S. Qing-feng, H. Guo, and J. Wang, Phys. Rev. B **65**, 075315 (2002); L. Dell Anna, A. Zazunov, R. Egger, and T. Martin, *ibid.* **75**, 085305 (2007).
[16] H. Haug, *Antti-Pekka Jauho, Quantum Kinetics in Transport and Optics of Semiconductors*, 1st ed. (Springer, New York, 1996), Chap. 12, p. 166.
[17] J. P. Perdew, K. Burke, and M. Ernzerhof, Phys. Rev. Lett. **77**, 3865 (1996).
[18] P. E. Blochl, Phys. Rev. B **50**, 17953 (1994).
[19] Qing-feng Sun, J. Wang, and Tsung-han Lin, Phys. Rev. B **59**, 3831 (1999).